AD-A179 706 UNSTEADY BOUNDARY LAYERS WITH AN INTELLIGENT NUMERICAL SCHEME(U) DOUGLAS AIRCRAFT CO LONG BEACH CA T CEBECI NOV 84 MDC-J3593 AFOSR-TR-87-0552 F49620-82-C-0055 1/1

UNCLASSIFIED F/G 20/4 NL

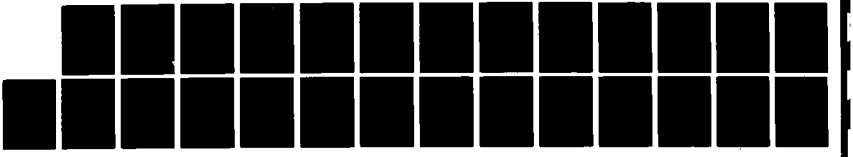

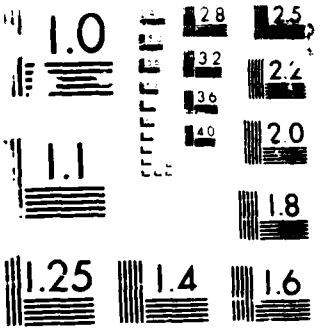
1.0
1.1
1.25
1.4
1.6
1.8
2.0
2.2
2.5
2.8
3.2
3.6
4.0

AD-A179 706

REPORT DOCUMENTATION PAGE

UNCLASSIFIED	1b. RESTRICTIVE MARKINGS
2a. SECURITY CLASSIFICATION AUTHORITY	3. DISTRIBUTION/AVAILABILITY OF REPORT Approved for Public Release; Distribution Unlimited.
2b. DECLASSIFICATION/DOWNGRADING SCHEDULE	
4. PERFORMING ORGANIZATION REPORT NUMBER(S) MDC J3593	5. MONITORING ORGANIZATION REPORT NUMBER(S) AFOSR-TR- 87-0552
6a. NAME OF PERFORMING ORGANIZATION McDONNELL DOUGLAS CORPORATION	6b. OFFICE SYMBOL (If applicable) DAC
7a. NAME OF MONITORING ORGANIZATION AFOSR/ Bolling AFB, DC 20332	
6c. ADDRESS (City, State and ZIP Code) Douglas Aircraft Company 3855 Lakewood Boulevard Long Beach, CA 90846	7b. ADDRESS (City, State and ZIP Code) AFOSR/ Bolling AFB, DC 20332
8a. NAME OF FUNDING/SPONSORING ORGANIZATION AIR FORCE OFFICE OF SCIENTIFIC RESEARCH	8b. OFFICE SYMBOL (If applicable) AFOSR/NA
8c. ADDRESS (City, State and ZIP Code) BET 4C Bolling AFB, DC 20332	9. PROCUREMENT INSTRUMENT IDENTIFICATION NUMBER F49620-82-C-0055
	10. SOURCE OF FUNDING NOS.

PROGRAM ELEMENT NO.	PROJECT NO.	TASK NO.	WORK UNIT NO.
61102F	2307	A2	

11. TITLE (Include Security Classification)
UNSTEADY BOUNDARY LAYERS WITH AN INTELLIGENT NUMERICAL SCHEME (U)

12. PERSONAL AUTHOR(S)
CEBECI, TUNCER

13a. TYPE OF REPORT	13b. TIME COVERED	14. DATE OF REPORT (Yr., Mo., Day)	15. PAGE COUNT
~~Interim~~ Final	FROM _____ TO _____	1984 NOVEMBER	21

16. SUPPLEMENTARY NOTATION

17 COSATI CODES		
FIELD	GROUP	SUB. GR

18. SUBJECT TERMS (Continue on reverse if necessary and identify by block number)
Flow reversal, Boundary layers, Unsteady boundary layers

19. ABSTRACT (Continue on reverse if necessary and identify by block number)

A numerical method has been developed to represent unsteady boundary layers with large flow reversal. It makes use of the characteristic box scheme which examines the finite-difference grid in relation to the magnitude and direction of local velocity and reaches and implements a decision to ensure that the Raetz principle of regions of influence and dependence is not violated. The method has been applied to the problem of an impulsively started circular cylinder and the results though generally consistent with those of van Dommelen and Shen obtained with a Lagrangian method, show some differences. The time step is identified as very important and, with the present intelligent numerical scheme, the results were readily extended to times far beyond those previously achieved with Eulerian methods. Extrapolation of the results suggests that the much discussed singularity for this unsteady flow is the same as that of the corresponding steady flow.

20. DISTRIBUTION/AVAILABILITY OF ABSTRACT	21. ABSTRACT SECURITY CLASSIFICATION
UNCLASSIFIED/UNLIMITED ☒ SAME AS RPT ☐ DTIC USERS ☐	UNCLASSIFIED

22a. NAME OF RESPONSIBLE INDIVIDUAL	22b. TELEPHONE NUMBER (Include Area Code)	22c. OFFICE SYMBOL
Dr. James D. Wilson	202/767-4935	AFOSR/NA

DD FORM 1473, 83 APR EDITION OF 1 JAN 73 IS OBSOLETE.

Unclassified
SECURITY CLASSIFICATION OF THIS PAGE

and Shen obtained with a Lagrangian method, show some differences. The time step is identified as very important and, with the present intelligent numerical scheme, the results were readily extended to times far beyond those previously achieved with Eulerian methods. Extrapolation of the results suggests that the much discussed singularity for this unsteady flow is the same as that of the corresponding steady flow.

AFOSR-TR- 87-0552

Copy number

Report number MDC J3593

UNSTEADY BOUNDARY LAYERS WITH AN INTELLIGENT NUMERICAL SCHEME

CRAD Final Report

Revision date

Revision letter

Issue date November 1984

Contract number F496720-82-C-0055

Prepared by: T. Cebeci

Approved for public release; distribution unlimited.

Approved by:

R. E. Pendley

R. E. Pendley
Director,
Aircraft Configuration & Performance

Accession For	
NTIS GRA&I	X
DTIC TAB	☐
Unannounced	☐
Justification	
By	
Distribution/	
Availability Codes	
Dist	Avail and/or Special
A-1	

AIR FORCE OFFICE OF SCIENTIFIC RESEARCH (AFSC)
NOTICE OF TRANSMITTAL TO DTIC
This technical report has been reviewed and is approved for public release IAW AFR 190-12.
Distribution is unlimited.
MATTHEW J. KERPER
Chief, Technical Information Division

DOUGLAS AIRCRAFT COMPANY

MCDONNELL DOUGLAS CORPORATION

TABLE OF CONTENTS

1.0 INTRODUCTION

Until recent work by van Dommelen and Shen (1981, 1982a), controversy existed with regard to the possibility that a singularity occurs at a finite time and position in an unsteady boundary layer evolving under prescribed pressure distribution. The consequences of its existence are large, particularly for the inviscid flow. It seems possible, however, that previous uncertainties have arisen from inability to accurately calculate unsteady flows with large reversal. For their calculations, van Dommelen and Shen made use of a Lagrangian formulation of the two-dimensional unsteady boundary-layer equations and considered a circular cylinder started impulsively from rest. They confirmed the existence of a singularity and the accuracy of their method. It is to be expected that the singularity will also exist in an Eulerian formulation but many previous attempts, for example, those of Belcher et al. (1971) and Telionis and Tsahalis (1974) have failed to reveal it. Useful reviews of the topic have been provided by Riley (1975), Williams (1977), Shen (1978), Telionis (1979) and Cebeci (1982).

With his Eulerian formulation, Cebeci (1979) performed calculations for the same problem. The results extended to $\tau = 2.8$ at which time they were terminated because the shear layers became too thick to be accurately represented by the numerical scheme. Also, a maximum and a minimum developed in the displacement thickness distribution and tended to cause the solutions to oscillate. Subsequent calculations with an improved transformation allowed solutions up to $\tau = 3.0$ but the nonmonotonic variations of the displacement thickness remained, Cebeci (1982). The results were in close agreement with those of van Dommelen and Shen (1982a) up to around $\tau = 2.75$.

Consideration of the above results led to a tentative conclusion that the numerical scheme was at fault and that previous Eulerian formulations may have had similar numerical shortcomings. Further calculations were performed to systematically investigate the influence of step lengths in time and x-direction and confirmed that the nonmonotonic variation of displacement thickness could be reduced by the use of smaller step lengths but an optimum relationship between Δt and Δx could not be determined and appeared essential. These calculations were performed with a form of Keller's Box method modified to include the zig-zag formulation of Krause et al. (1968). In common with

the often-used Crank-Nicolson method (1947), this scheme is convenient, particularly since the orientation of the numerical mesh is chosen a priori. This advantage has a corresponding and potentially dangerous drawback in the presence of large reverse flows. The precise boundaries of the solution domain must obey the Raetz theory (1957) of influence-regions and the zones of influence and dependence may not be properly represented. This potential defect can be overcome only by ensuring that the mesh is correctly aligned with the flow direction and thereby allows the local flow properties to be correctly influenced by its neighbors.

Here we describe a new numerical scheme which is intelligent in the sense that it examines the choice of grid in relation to the magnitude and direction of the local velocity and reaches and implements a decision which ensures that Raetz's theory is obeyed. It is applied to the time dependent equations of the following section and makes use of a form of the characteristic box described in Section 3.0. The results for an impulsively started circular cylinder are presented and discussed in Section 4.0.

2.0 BASIC EQUATIONS

We consider incompressible unsteady laminar flow over a circular cylinder started impulsively from rest. The governing boundary-layer equations and their boundary conditions for this flow are well known, see for example, Cebeci (1979) and are given by

$$\frac{\partial u}{\partial x} + \frac{\partial v}{\partial y} = 0 \tag{1}$$

$$\frac{\partial u}{\partial t} + u\frac{\partial u}{\partial x} + v\frac{\partial u}{\partial y} = u_e\frac{du_e}{dx} + \nu\frac{\partial^2 u}{\partial y^2} \tag{2}$$

$$y = 0, \qquad u = v = 0; \qquad y \to \infty, \qquad u \to u_e(x) \tag{3}$$

To generate the initial conditions for the above equations at $t = 0$ and to put them into a more convenient form for solution, we define the similarity variable η and a dimensionless stream function $f(x,\eta,\tau)$ by

$$\eta = \left(\frac{u_o}{\nu L\tau}\right)^{1/2} y, \qquad f(\bar{x},\eta,\tau) = \frac{\psi}{(\nu u_o L\tau)^{1/2}\,\bar{u}_e} \tag{4}$$

where ψ is the usual definition of stream function which satisfies Eq. (1), u_o denotes a reference velocity $2\pi u_\infty$, L is a reference length equal to πa with a corresponding to the cylinder radius, τ is a dimensionless time equal to $u_o t/L$, $\bar{u}_e$ is a dimensionless velocity, u_e/u_o and $\bar{x} = x/L$. In terms of these relations, with primes denoting differentiation with respect to η, Eqs. (1) to (3) can be written as

$$f''' + \frac{\eta}{2}f'' + \tau\frac{d\bar{u}_e}{d\bar{x}}[1 - (f')^2 + ff''] = \tau\left[\frac{\partial f'}{\partial\tau} + \bar{u}_e\left(f'\frac{\partial f'}{\partial\bar{x}} - f''\frac{\partial f}{\partial\bar{x}}\right)\right] \tag{5}$$

$$\eta = 0, \qquad f = f' = 0; \qquad \eta = \eta_e, \qquad f' = 1 \tag{6}$$

These variables are employed only in the interval during which the boundary layer develops rapidly. At higher values of time, the exponential-like growth of the boundary-layer thickness with time near the rear stagnation point region, is represented in terms of the dimensionless variables Y and F defined by

$$Y = \left(\frac{u_o}{\nu L}\right)^{1/2} y e^{1-\tau}, \qquad \psi = (\nu u_o L)^{1/2} e^{\tau-1} \bar{u}_e F(\bar{x}, Y, \tau) \tag{7}$$

and Eqs. (1)-(3) become

$$F''' + b\eta F'' + b\frac{d\bar{u}_e}{d\bar{x}}[1 - (F')^2 + FF''] = b\frac{\partial F'}{\partial \tau} + b\bar{u}_e\left[F'\frac{\partial F'}{\partial \bar{x}} - F''\frac{\partial F}{\partial \bar{x}}\right] \tag{8}$$

$$Y = 0, \qquad F = F' = 0; \qquad Y = Y_e, \qquad F' = 1 \tag{9}$$

Here $b = e^{2(\tau-1)}$ and the primes denote differentiation with respect to Y.

Equations (5) and (8) can also be expressed in the common form:

$$f''' + b_1\eta f'' + b\frac{d\bar{u}_e}{d\bar{x}}[1 - (f')^2 + ff''] = b\frac{\partial f'}{\partial \tau} + b\bar{u}_e\left(f'\frac{\partial f'}{\partial \bar{x}} - f''\frac{\partial f}{\partial \bar{x}}\right) \tag{10}$$

where, with $f = F$ for $\tau \leq \tau_*$

$$b_1 = \begin{cases} 1/2 & \tau \leq \tau_* \\ e^{2(\tau-1)} & \tau > \tau_* \end{cases} \qquad b = \begin{cases} \tau & \tau \leq \tau_* \\ b_1 & \tau > \tau_* \end{cases}$$

The initial conditions at t = 0 can be obtained from Eq. (10) which reduces to

$$f''' + \frac{1}{2}\eta f'' = 0 \tag{11}$$

and whose solution, subject to Eq. (6), is given by

$$f = \eta\,\mathrm{erf}\left(\frac{\eta}{2}\right) + \frac{2}{\sqrt{\pi}}\left[\exp\left(-\frac{\eta^2}{4}\right) - 1\right] \tag{12}$$

The initial conditions along the (τ,η) plane at the forward and rear stagnation points can also be obtained from Eq. (10). If the external velocity distribution is represented by

$$\bar{u}_e = \frac{1}{\pi}\sin(\pi\bar{x}) \tag{13}$$

then at $\bar{x} = 0$ and 1, Eq. (10) becomes

$$f''' + b_1\eta f'' + b\lambda[1 - (f')^2 + ff''] = b\frac{\partial f'}{\partial \tau} \tag{14}$$

where $\lambda = 1$ for $\bar{x} = 0$ and $\lambda = -1$ for $\bar{x} = 1$.

3.0 NUMERICAL METHOD

The solution of the time-dependent boundary-layer equations with no flow reversal in u across the layer is routine and can be achieved easily with the Keller (1974) or Crank-Nicolson method (1947). These procedures are described in several references, see for example, Bradshaw et al. (1981). When there is flow reversal, however, the solution of the time-dependent boundary-layer equations is not straightforward and requires special procedures to avoid the numerical instabilities. The zig-zag formulation of Krause et al. (1968) helps to remedy the difficulties but is not sufficient in all cases, as we shall discuss later. An accurate and physically sound numerical method is the characteristic scheme developed for three-dimensional steady boundary-layer flows by Cebeci and Stewartson (1978) which is based on the solution of governing equations along local streamlines. It allows the step sizes in the t and x directions to be automatically adjusted to ensure that the region of backflow determined by the local streamlines does not violate Raetz's regions of influence. A brief description of this method for the problem of the impulsively started cylinder is given below.

We first define a new variab θ by

$$\theta = b \frac{d\bar{u}_e}{d\bar{x}} f + b\bar{u}_e \frac{\partial f}{\partial \bar{x}} \tag{15}$$

and write Eq. (10) as

$$f''' + b_1 \eta f'' + \theta f'' + b \frac{d\bar{u}_e}{d\bar{x}} [1 - (f')^2] = b \frac{\partial f'}{\partial \tau} + b\bar{u}_e f' \frac{\partial f'}{\partial \bar{x}} \tag{16}$$

One of the basic ideas of Keller's box method is to write Eq. (16) in the form of a first-order system. For this purpose we denote f' by g, let

$$g' = w \tag{17}$$

and write Eqs. (15) and (16) and their boundary conditions as

$$\theta' = b \frac{d\bar{u}_e}{d\bar{x}} g + b\bar{u}_e \frac{\partial g}{\partial \bar{x}} \tag{18}$$

$$w' + b_1 \eta w + \theta w + b \frac{d\bar{u}_e}{d\bar{x}} (1 - g^2) = b \frac{\partial g}{\partial \tau} + b\bar{u}_e g \frac{\partial g}{\partial \bar{x}} \tag{19}$$

$$\eta = 0, \qquad \theta = g = 0; \qquad \eta = \eta_e, \qquad g = 1. \tag{20}$$

The solution of the system given by Eqs. (17) to (20) by the standard or characteristic box methods depends on how the difference equations are written for Eq. (19); the remaining equations are unchanged. In the following paragraphs we first consider Eqs. (17) and (18) and show how the difference equations are written.

Consider the net cube shown in Fig. 1 and denote the net points by

$$\begin{aligned} \bar{x}_0 &= 0, & \bar{x}_i &= \bar{x}_{i-1} + r_i & i &= 1, 2, \ldots, I \\ \tau_0 &= 0, & \tau_n &= \tau_{n-1} + k_n & n &= 1, 2, \ldots, N \\ \eta_0 &= 0, & \eta_j &= \eta_{j-1} + h_j & j &= 1, 2, \ldots, J \end{aligned} \tag{21}$$

where $r_i = \Delta\bar{x}_i$, $k_n = \Delta\tau_n$ and $h_j = \Delta\eta_j$.

The difference approximations that are to represent Eq. (17) are obtained by averaging about the midpoint $(\bar{x}_i, \tau_n, \eta_{j-1/2})$,

$$h_j^{-1}(g_j^{i,n} - g_{j-1}^{i,n}) = w_{j-1/2}^{i,n} \tag{22}$$

where, for example,

$$w_{j-1/2}^{i,n} = 1/2 \, (w_j^{i,n} + w_{j-1}^{i,n}) \tag{23}$$

The difference approximations to Eq. (18) are obtained by centering all quantities except θ at the center of the cube $(\bar{x}_{i-1/2}, \tau_{n-1/2}, \eta_{j-1/2})$ by

taking the values of each variable, say q, at the four corners of the box, that is,

$$q_{j-1/2}^{i-1/2,n} = \frac{1}{2}\left(q_{j-1/2}^{i,n} + q_{j-1/2}^{i-1,n}\right) = \frac{1}{4}\left(q_j^{i,n} + q_j^{i-1,n} + q_{j-1}^{i,n} + q_{j-1}^{i-1,n}\right) \quad (24a)$$

However, the centering of θ is done by writing it as

$$\theta_{j-1/2}^{i-1/2,n-1/2} = \frac{1}{2}\left(\theta_j^{i-1/2,n-1/2} + \theta_{j-1}^{i-1/2,n-1/2}\right) \quad (24b)$$

In terms of this notation, the finite-difference approximations to Eq. (18) can be written in the following form:

$$h_j^{-1}(\theta_j - \theta_{j-1}) - \left(b\frac{d\bar{u}_e}{d\bar{x}}\right)^{i-1/2,n-1/2} \bar{g}_{j-1/2}$$

$$= (b\bar{u}_e)^{i-1/2,n-1/2} r_i^{-1}(\bar{g}_i - \bar{g}_{i-1}) \quad (25)$$

where, for example,

$$\theta_j = \theta_j^{i-1/2,n-1/2}, \qquad \bar{g}_j = \frac{1}{2}\left(g_j^{i-1/2,n} + g_j^{i-1/2,n-1}\right), \quad (26)$$

The unknown variables in Eq. (25) correspond to $g_j^{i,n}$ and $\theta_j^{i-1/2,n-1/2}$ so that when a solution of the system given by Eqs. (17) to (20) is obtained, g is computed at (i,n,j) and θ at (i-1/2,n-1/2,j). This modified centering procedure is necessary to avoid oscillations due to the use of the continuity equation in the form given by Eq. (15) rather than the use of the stream function which allows continuity and momentum equations to be expressed as a third-order equation.

With the standard box scheme, the difference approximations corresponding to Eq. (19) is formulated in the same way as has been described above. With the characteristic box, however, an alternative procedure is followed and is described below. This scheme is based on the solution of the governing equations along the local streamlines defined by

$$\frac{d\bar{t}}{\bar{T}} = \frac{d\bar{x}}{g\bar{u}_e} \quad (27)$$

If we denote distance in this direction by ξ and the angle that it makes with the τ-axis by β, then Eq. (19) can be written as

$$w' + b_1 \eta w + \theta w + b \frac{d\bar{u}_e}{d\bar{x}} (1 - g^2) = \lambda \frac{\partial g}{\partial \xi} \tag{28}$$

where

$$\lambda = b\sqrt{1 + (\bar{u}_e g)^2} \tag{29a}$$

$$\beta = \tan^{-1} u \tag{29b}$$

The finite-difference approximations to Eq. (28) are written along the streamline direction (see Fig. 2). The resulting expressions are lengthy and to illustrate the procedure, we consider the model equation,

$$w' + \theta w = \lambda \frac{\partial g}{\partial \xi} \tag{30}$$

With the notation shown in Fig. 2, the difference approximations to Eq. (30) at point P are

$$\frac{h_j^{-1}}{2} (w_j^{i,n} - w_{j-1}^{i,n}) + \frac{h_j^{-1}}{2} (w_j^{s,n-1} - w_{j-1}^{s,n-1}) + \theta^P_{j-1/2} \frac{1}{2} (w^{i,n}_{j-1/2} + w^{s,n-1}_{j-1/2})$$

$$= \frac{1}{2} (\lambda^{i,n}_{j-1/2} + \lambda^{s,n-1}_{j-1/2}) \frac{g^{i,n}_{j-1/2} - g^{s,n-1}_{j-1/2}}{\Delta \xi_j} \tag{31}$$

where the relation between $\theta^P_{j-1/2}$ and those values of θ centered at (i-1/2, n-1/2) and (i-3/2,n-1/2) are

$$\theta^P_{j-1/2} = \frac{\theta^{i-3/2}_{j-1/2} - \theta^{i-1/2}_{j-1/2}}{\bar{x}_{i-3/2} - \bar{x}_{i-1/2}} (\bar{x}^P - \bar{x}_{i-3/2}) + \theta^{i-3/2}_{j-1/2} \tag{32}$$

The boundary conditions follow from Eqs. (9) and can be written as

$$g_0 = \theta_0 = 0; \qquad g_J = 1 \tag{33}$$

The algebraic system given by Eqs. (22), (25) and (31) together with the boundary conditions given by Eq. (33) is nonlinear. Linearization is achieved

with Newton's method and the equations are then solved by the block-elimination described, for example, in Bradshaw et al. (1981).

In the calculations described in the next section, the standard box scheme has been used for all situations when there is no flow reversal. Where a calculation with the standard box reveals a flow reversal ($u_j < 0$) further iterations at that location make use of the characteristic scheme for $u_j < 0$ and the standard box for $u_j > 0$. This switch from one scheme to another continues to allow quadratic convergence and ensures that, provided the step lengths in the τ and $\bar{x}$ directions are "properly" selected, the numerical instabilities are avoided. Further details are provided in the next section.

4.0 RESULTS

It is convenient to present the results which we have obtained using the combination of standard and characteristic box schemes and then to discuss them in relation to previous calculations. Finally, the numerical requirements of the present results are discussed together with the implications of the results for future calculations of more realistic unsteady flows.

Figures 3,4 and 5 display the variations of dimensionless displacement thickness, Δ^*, local skin-friction coefficient, c_f and displacement velocity, $\bar{v}_w$ where these are defined, with $R_L = u_o L/\nu$, by

$$\Delta^* = \frac{\sqrt{R_L}}{L} \int_0^\delta (1 - \frac{u}{u_e}) dy$$

$$c_f^* = \frac{2\tau_w}{\rho u_o^2} \sqrt{R_L} \tag{34}$$

$$\bar{v}_w = \frac{v_w}{u_o} = \frac{d}{d\bar{x}} (\bar{u}_e \Delta^*)$$

It is of particular note that the displacement thickness is close to monotonic with the small maximum and minimum for $\tau = 3.1$ at which the calculations were terminated. The previous results of Cebeci (1982) are also shown in the figure and reveal the maxima which stemmed from the use of a numerical scheme which did not meet the requirements imposed by the Raetz principle.

The distributions of local skin-friction coefficients of Fig. 4 show trends which are similar to those of the previous results but with differences in magnitude consistent with those of Fig. 3. It should be noted that the results of Figs. 3 and 4 are identical with those previously obtained up to the value of θ at which the displacement thickness gradient reaches its maximum and for values of τ less than around 2.75. The differences for large values of θ and τ are associated with the numerical procedure and, in particular, with its ability to satisfy the Raetz principle as is discussed later.

The dimensionless displacement velocity, $\bar{v}_w$, is shown in Fig. 5 together with the locus of points corresponding its maxima which increases with time and decreasing angle. At $\tau = 3.0$, the calculated value of θ is 111.5 and corresponds very closely to that determined by van Dommelen and Shen who terminated their calculations at this time. As the peak in the displacement velocity moves upstream with increasing time, the location at which the skin-friction coefficient becomes zero also moves upstream but at a slower rate and towards its steady-state value of 105°, Cebeci and Smith (1974). It may be conjectured that the extrapolation of the peak displacement velocities will asymptote to this steady-state value but positive confirmation will require excessive computer resources.

Corresponding velocity profiles are presented in Fig. 6 for $\tau = 2.75$ and 3.0. The general trends are in agreement with those of van Dommelen and Shen and that the quantitative values agree closely up to 110°. The discrepancies at larger angles are probably due to the use of inappropriate time steps in the calculations. The previous results of Cebeci (1982) tended to agree with the profiles of van Dommelen and Shen as shown in figure 6a and are thought to be inaccurate as is discussed in the following section.

5.0 CONCLUDING REMARKS

The previous calculations of Cebeci (1982) were terminated because it proved to be impossible to select the step lengths required to satisfy the Raetz's criteria in the presence of large flow reversal. Other attempts to make use of Eulerian formulations to calculate unsteady flows with large backflow have been plagued with the same difficulty. The need for a measure which would ensure that the Raetz principle was satisfied has been met in the present calculations. Here the calculations were performed at a given time and with the step lengths in x chosen to have the values shown in Table 1. As can be seen, the values of Δx are very much smaller in the vicinity of singularity. The solutions were iterated at each x-station until a convergence criterion based on the wall shear parameter f_w'' was satisfied, that is,

$$\left| (f_w'')^{\nu+1} - (f_w'')^{\nu} \right| < \delta_1 \tag{35}$$

where δ_1 is a tolerance parameter which was set equal to 10^{-5} in the calculations.

The keys to the success of the present approach lie in the characteristic box scheme which allows the orientation of the finite-difference mesh to vary across the shear layer and the procedure for the automatic selection of time steps so as to maintain the angle

$$\beta < \tan^{-1} \frac{r_i}{k_n} \tag{36}$$

The value of k_n was halved until this condition was met. The resulting values of k_n are also shown in Table 1 and can be seen to become extremely small at $\tau = 3.0$. The present calculations which made use of increments in $\bar{x}$,Y and τ of 101, 161 and 435, respectively, could have been extended beyond $\tau = 3.1$ but at considerable expense as witnessed by the small and decreasing values of k_n. The values of k_n and r_i shown in Table 1 were subsequently used in conjunction with the zig-zag scheme, which had previously failed, Cebeci (1982), to permit calculations for time greater than $\tau > 2.75$. The results were found to be identical to those presented here. The alternative approach of using the zig-zag scheme and the relationship given by Eq. (36) was not, however, successful. This confirms that it is necessary to allow the flow direction to change across the layer by conditions determined by the local streamlines in the selection of k_n.

Table 1. The distribution of step sizes in τ and $\bar{x}$.

τ	k_n	$\bar{x}$	r_i
0 → 1	0.05	0 → 0.54	0.02
1 → 1.5	0.02	0.54 → 0.57	0.01
1.5 → 2.3	0.01	0.57 → 0.58	0.0025
2.3 → 2.73	0.005	0.58 → 0.60	0.0020
2.73 → 3.024	0.002	0.60 → 0.612	0.0015
3.024 → 3.1	0.001	0.612 → 0.64	0.0020
		0.64 → 0.67	0.0025
		0.67 → 0.72	0.01
		0.72 → 1.0	0.02

It is clear that our new procedure has successfully permitted the calculation of the flow properties for the unsteady flow associated with a cylinder impulsively started from rest. The large reverse flow regions found with this model problem occur in the more practical application of oscillating airfoils. Preliminary work has been carried out for this problem and has confirmed that this is so. In particular, the use of the characteristic box scheme together with Eq. (36) led to solutions which approached and past the region of the singularity without numerical difficulty whereas the zig-zag scheme led to solutions which oscillated and broke down in the same manner experienced with the cylinder.

The above discussion makes it clear that the time step required to obtain results at the larger values of τ are very small as was concluded by Ingham (1984). For this reason, the present calculations were terminated at $\tau = 3.1$ which is already larger than that of previous investigators. Fig. 5 shows that it is desirable to perform calculations at higher values of τ so as to confirm the conjecture that the only singularity is associated with the steady-state solution. To make a conclusive judgment, calculations should be performed up to $\tau = 4.1$ but, as Table 1 suggests, the required time steps are likely to be very small. The time required to obtain results in the range $\tau = 3.024$ to 3.1, which corresponds to 75 time-steps, was 7 hours on a CYBER 175. The computer time likely to be required to reach $\tau = 4.1$ is clearly excessive.

6.0 REFERENCES

Belcher, R.J., Burggraf, O.R., Cooke, J.C., Robins, A.J. and Stewartson, K. (1971), Limitless boundary layers, Recent Research on Unsteady Boundary Layers, Proc. Int. Union Theoret. Appl. Mech (E.A. Eichelbrenner, ed.), 1444-1466.

Bradshaw, P., Cebeci, T. and Whitelaw, J.H. (1981), Engineering Calculation Methods for Turbulent Flows, Academic Press, London.

Cebeci, T. (1979), The laminar boundary layer on a circular cylinder started impulsively from rest, J. Comp. Phys. 31, 153-172.

Cebeci, T. (1982), Unsteady separation, Numerical and Physical Aspects of Aerodynamic Flows (T. Cebeci, ed.), Springer-Verlag, NY, 265-277.

Cebeci, T. and Smith, A.M.O. (1974), Analysis of Turbulent Boundary Layers, Academic Press, NY.

Cebeci, T, and Stewartson, K. (1978), Unpublished work.

Crank, J. and Nicolson, P. (1947), A practical method of numerical evaluation of solutions of partial-differential equations of the heat-conduction type, Proc. Cambridge Phil. Soc. 43, 50.

Ingham, D.B. (1984), Unsteady separation. J. Comp. Phys. 53, 90-99.

Keller, H.B. (1974), Accurate difference methods for two-point boundary-value problems. SIAM J. Numer. Anal. 11 305-320.

Krause, E., Hirschel, E.H. and Bothmann, Th. (1968), Die numerische integration der bewegungsgleichungen dreidimensionaler laminarer kompressibler grenzschichten, Bond 3, Fachtagung Aerodynamik, Berlin; D6LR-Fachlinchreike.

Raetz, G.S. (1957), A method of calculating three-dimensional laminar boundary layers of steady compressible flows, Northrop Corp. Rept. No. NAI 58-73.

Riley, N. (1975), Unsteady laminar boundary layers, SIUAM Rev. 17, 274.

Sears, W.R. and Telionis, D.P. (1975), Boundary-layer separation in unsteady flow, SIAM J. Appl;. Math 28, 215.

Shen, S.F. (1978), Unsteady separation according to the boundary-layer equations. Advances in Applied Mecn. 18, 177-200.

Telionis, D.P. (1979), Review - Unsteady boundary layers, separated and attached. J. Fluids Eng. 101, 29-43.

Telionis, D.P. and Tsahalis, D.T. (1974), Unsteady laminar separation over cylinder started impulsively from rest, Acta Astronautics 1, 1487.

van Dommelen, L.L. and Shen, S.F. (1981), The spontaneous generation of the singularity in a separating laminar boundary layer. J. Comp. Phys. 38, 125-140.

van Dommelen, L.L. and Shen, S.F. (1982a), The genesis of separation, Numerical and Physical Aspects of Aerodynamic Flows (T. Cebeci, ed.), Springer-Verlag, NY, 293-311.

van Dommelen, L.L. and Shen, S.F. (1982b), Private communication.

Williams, J.C., III (1977), Annual Rev. Fluid Mech. 9.

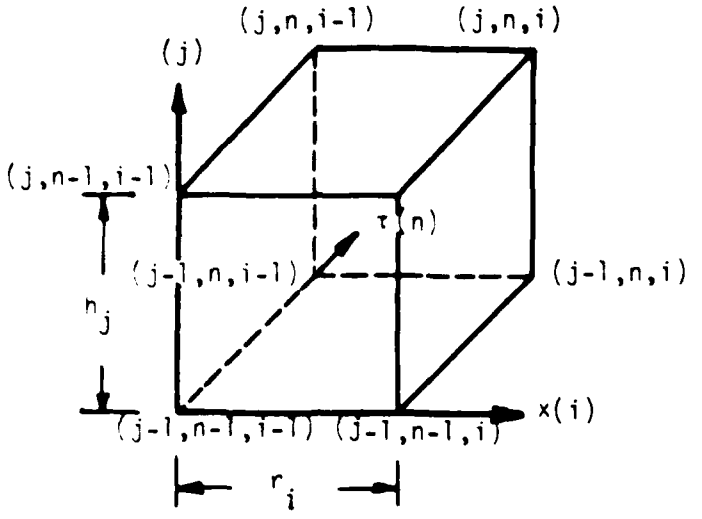

Figure 1. Net cube for the difference equations.

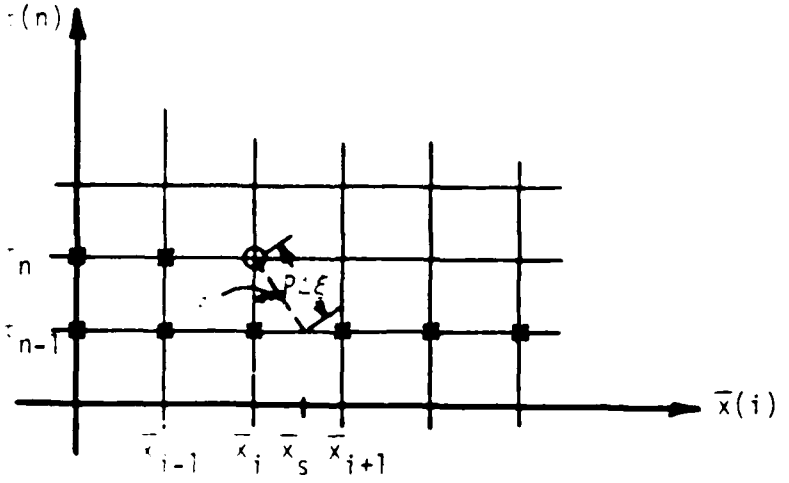

Figure 2. Notation for the characteristic box scheme

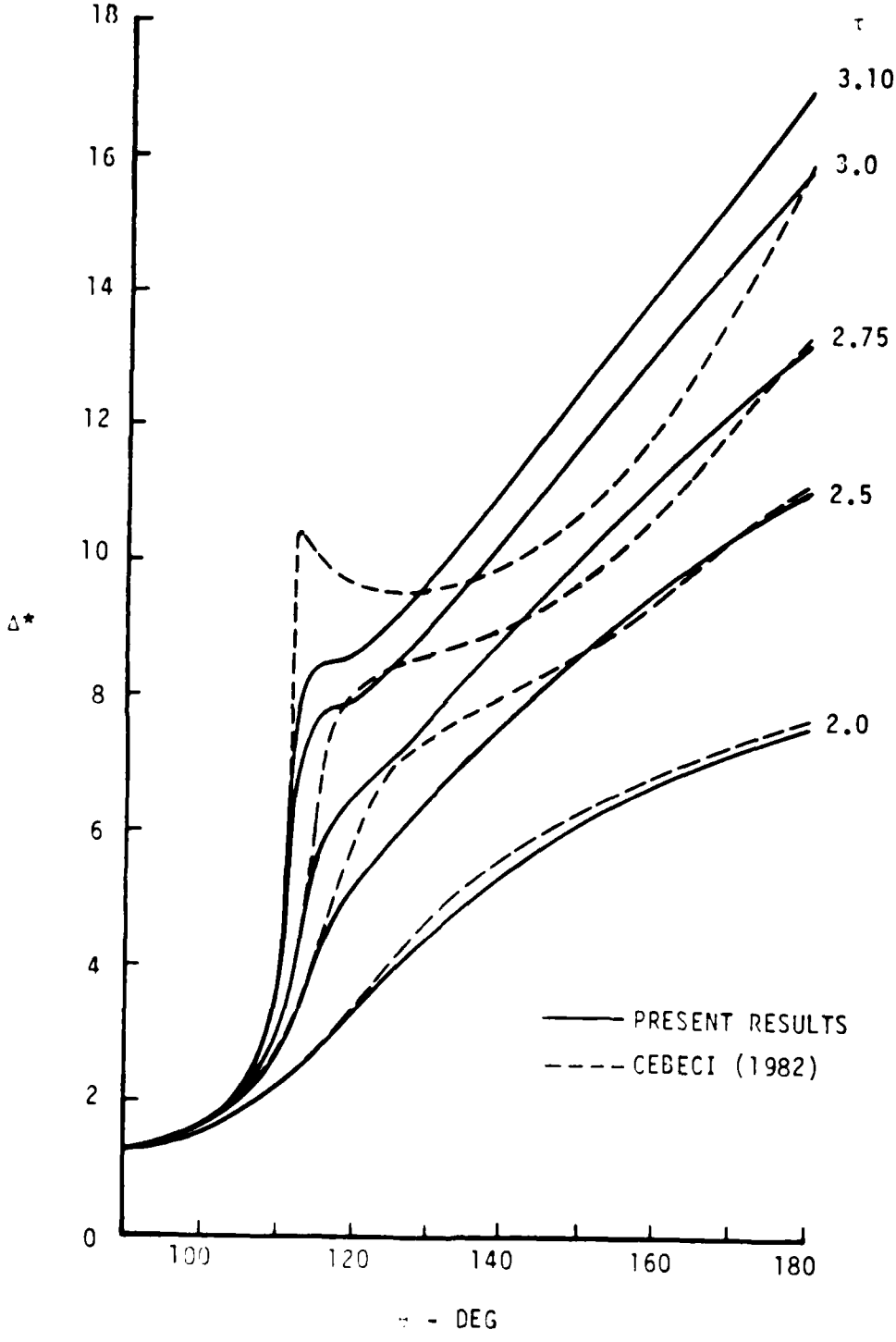

Figure 3. Variation of dimensionless displacement thickness

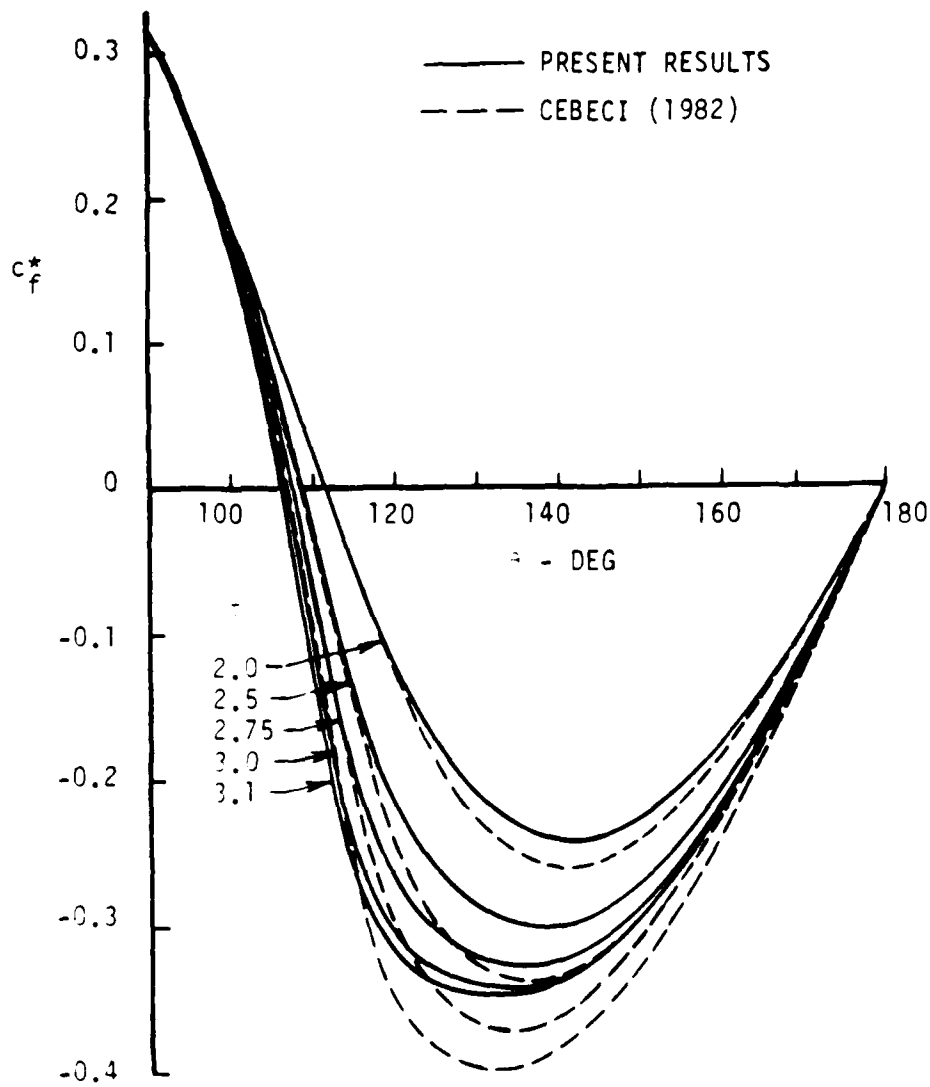

Figure 4. Variation of dimensionless local skin friction coefficient.

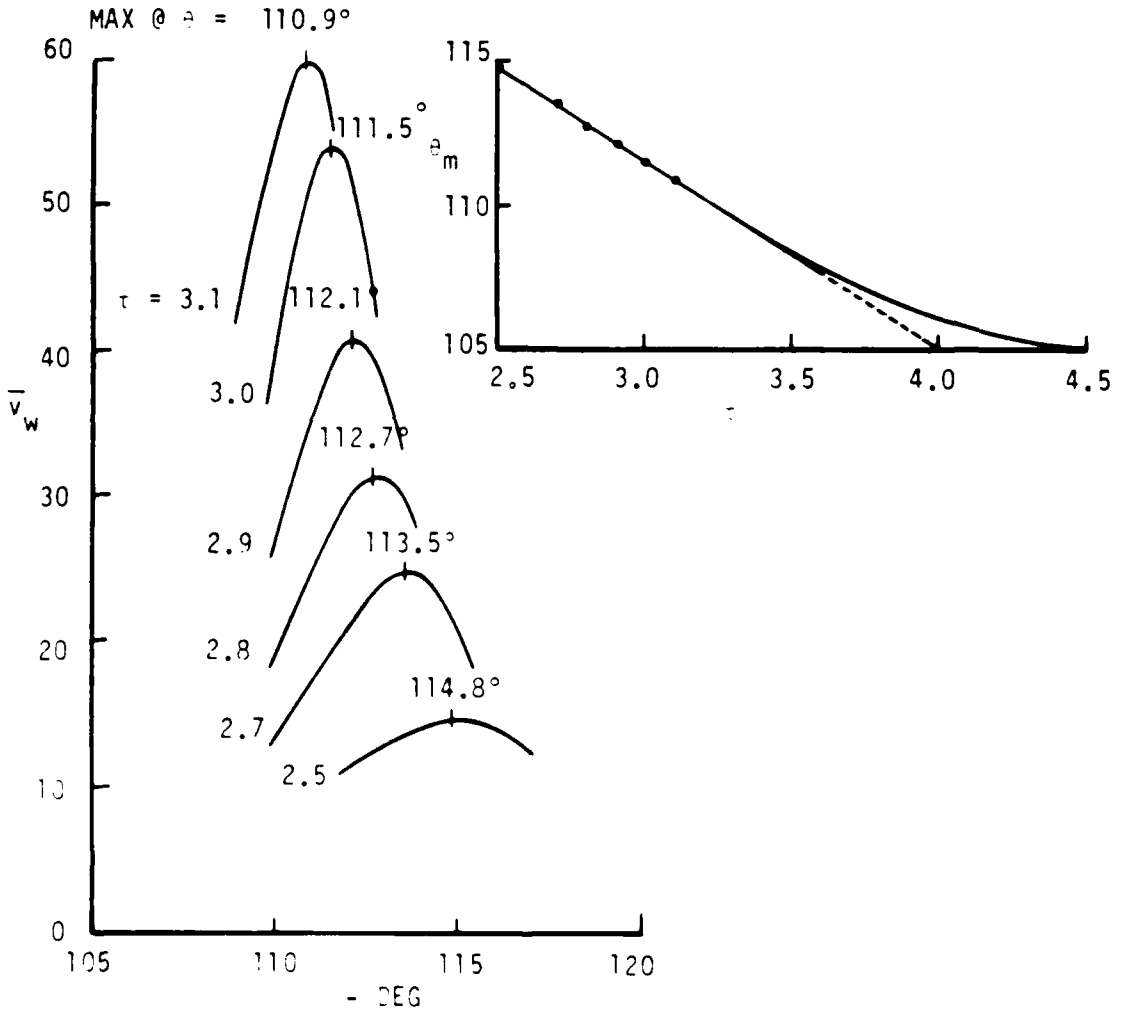

Figure 5. Variation of dimensionless displacement velocity. The insert shows the variation of the location of maximum displacement velocity θ_m with circles indicating the computed values, the dashed lines indicate the linear extrapolation of θ_m and the solid line a conjectured variation of θ_m to steady state.

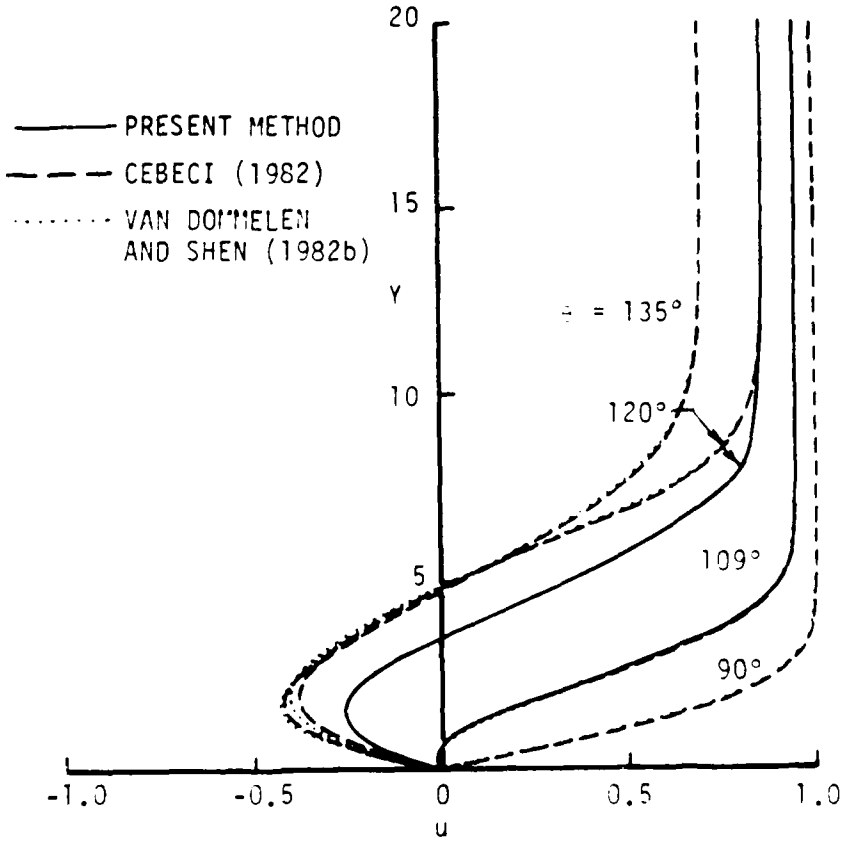

Figure 6. Velocity profiles at different times. (a) = 2.75.

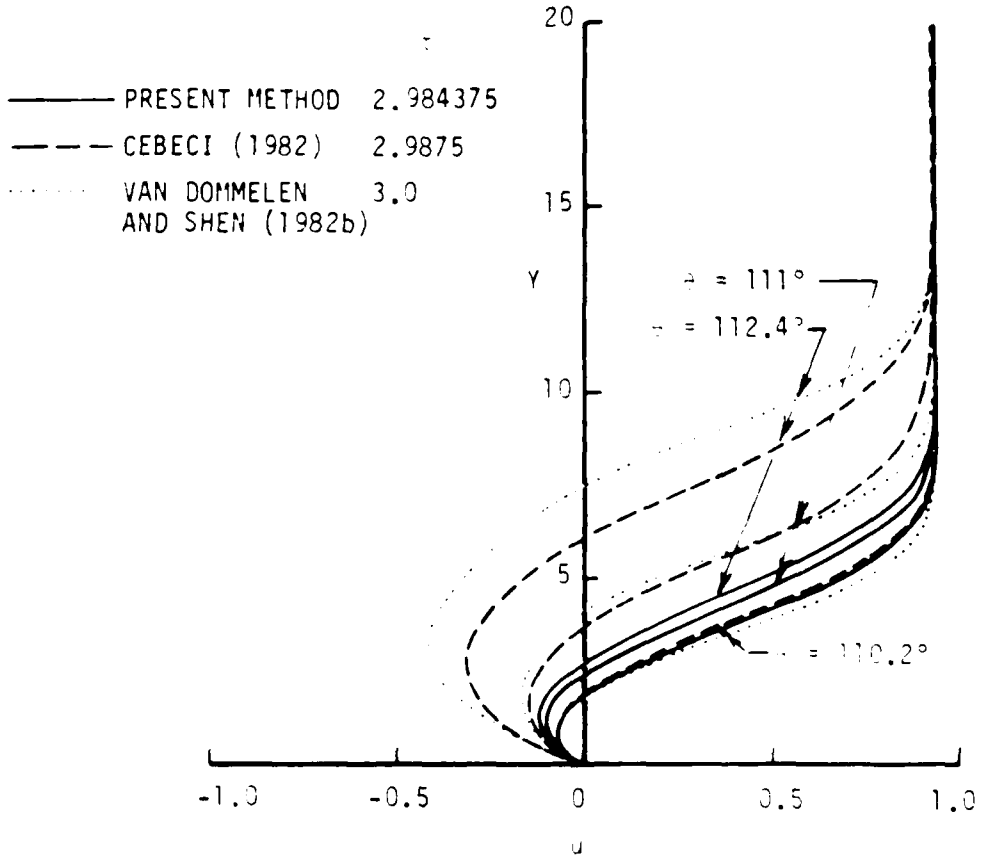
PRESENT METHOD 2.984375
CEBECI (1982) 2.9875
VAN DOMMELEN AND SHEN (1982b) 3.0
20
15
10
5
Y
= 111°
= 112.4°
= 110.2°
-1.0
-0.5
0
0.5
1.0
u

Figure 6(b).

END

5-87

DTIC